



Soil properties modulate actual evapotranspiration and precipitation impacts on crop yields in the USA

Mahmoud Suliman^{a,*}, Anna Scaini^{b,c}, Stefano Manzoni^{b,c}, Giulia Vico^d

^a Department of Crop Production Ecology, the Swedish University of Agricultural Sciences, SE-750 07 Uppsala, Sweden

^b Department of Physical Geography, Stockholm University, Stockholm SE-106 91, Sweden

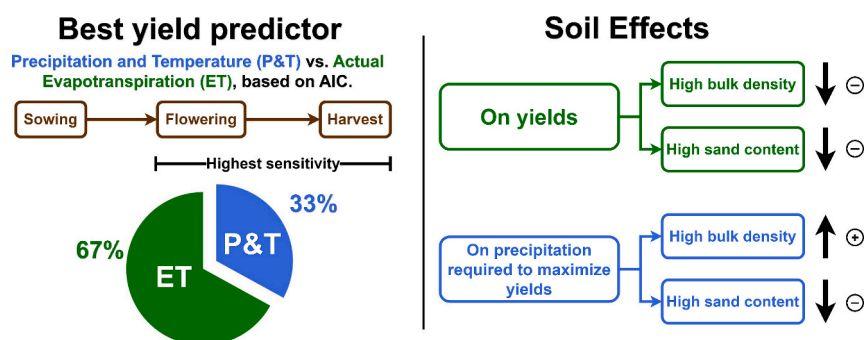
^c Bolin Centre for Climate Research, Stockholm University, Stockholm SE-106 91, Sweden

^d Department of Ecology, the Swedish University of Agricultural Sciences, SE-750 07 Uppsala, Sweden

HIGHLIGHTS

- We modeled yield variation for several staple crops over a broad range of interacting hydroclimatic and edaphic conditions.
- Actual evapotranspiration explained yield variations better than precipitation and temperature.
- Sandy soils needed less precipitation to maximize yields, suggesting effects akin to the inverse texture hypothesis.
- Higher bulk density reduced yields and increased precipitation required for maximum yields
- Yields were generally most sensitive to changes in hydroclimatic conditions after flowering or silks emergence.

GRAPHICAL ABSTRACT



ARTICLE INFO

Editor: Alessandra De Marco

Keywords:

Crop yield
Evapotranspiration
Hydroclimatic impacts
Soil texture
Bulk density
Developmental phase

ABSTRACT

Crop yields are affected by hydroclimatic and edaphic conditions, but their interacting roles are often neglected when assessing crop yields at the regional scale. Moreover, often used hydroclimatic conditions such as precipitation and temperature are not as physiologically linked to primary production and yields as actual evapotranspiration. Using statistical models, we quantified the combined effects of edaphic and hydroclimatic conditions on county yields of irrigated rice and rainfed corn, soybean, and spring and winter wheat in the USA (2000–2019). Precipitation and temperature, or actual evapotranspiration, aggregated during the growing season or before and after flowering/silk emergence, in interaction with soil sand content or bulk density, explained up to 87 % of the yield variability. However, actual evapotranspiration explained yields better than precipitation and temperature and their interactions for most combinations of crops and growth periods. At high actual evapotranspiration, yield plateaued or, for spring wheat, decreased. Yields were generally most sensitive to changes in hydroclimatic conditions during part of rather than the entire growing season, and most often after

Abbreviations: ET, Actual Evapotranspiration; SC, Sand Content; BD, Bulk Density; P, Precipitation; T, Temperature; ETS, the Simplified Surface Energy Balance Actual Evapotranspiration; ETE, Actual Evapotranspiration from the ERA5-Land Hourly data; AGDD, Accumulated Growing Degree Days; GS, Growing Season; DP, Developmental Phase; DOY, Day of the Year; LME, Linear Mixed-effect; SI, Supplementary Information.

* Corresponding author.

E-mail addresses: mahmoud.suliman@slu.se (M. Suliman), anna.scaini@natgeo.su.se (A. Scaini), stefano.manzoni@natgeo.su.se (S. Manzoni), giulia.vico@slu.se (G. Vico).

<https://doi.org/10.1016/j.scitotenv.2024.175172>

Received 8 May 2024; Received in revised form 17 July 2024; Accepted 29 July 2024

Available online 31 July 2024

0048-9697/© 2024 The Authors. Published by Elsevier B.V. This is an open access article under the CC BY license (<http://creativecommons.org/licenses/by/4.0/>).

flowering. Soil texture and bulk density modulated the impacts of hydroclimatic conditions: corn and soybean yields were higher in finer soils compared with sandy soils under high evapotranspiration, but lower at low evapotranspiration. Additionally, the yield-maximizing precipitation decreased with sand content and increased with bulk density for most crops. Increasingly available actual evapotranspiration estimates, combined with soil properties, offer an alternative, and more physiologically-based, yield predictor over large climatic gradients to the more widely used precipitation and temperature.

1. Introduction

Global food security requires consistent yields of staple crops such as corn, wheat and rice (Elert, 2014). Globally, up to a third of yield fluctuations can be explained by climate variations (Ray et al., 2015). Crops are negatively affected by adverse hydroclimatic conditions (Hall et al., 2017), in particular when they co-occur. For instance, combined heat waves and droughts cause substantial crop losses (Brás et al., 2021). Moreover, given the importance of soil water and nutrient availability for plants, soil properties linked to water and nutrient cycling influence how hydroclimatic conditions affect yields (Ma et al., 2023). Yet, how hydroclimatic conditions interact with edaphic factors in shaping yield variations and responses to their changes remains uncharacterized over large areas and climatic gradients.

Crop growth and ultimately marketable yields depend on the cumulated carbon dioxide assimilation over the growing season. In turn, carbon dioxide assimilation rates are proportional to transpiration rates, as both carbon dioxide and water vapor are exchanged through the leaf stomata. As such, remotely sensed estimates of actual evapotranspiration (ET) are expected to be intimately related to plant carbon uptake, growth and, for crops, yields. ET is also an important indicator of crop water requirements and use (Goyal and Harmsen, 2013). On the one hand, ET is driven by air temperature providing energy for evaporation, and by soil water availability, replenished by precipitation or irrigation (Allen et al., 1998; Katul et al., 2012). On the other hand, ET drives the rate of soil water uptake by the plants, and hence the soil water balance (Rodríguez-Iturbe and Porporato, 2005; Wang et al., 2021). ET can thus summarize the effects of water availability from precipitation and irrigation, and of temperature on plant physiology and transpiration. Given the direct or indirect linkages between ET and virtually all plant processes, it is perhaps not surprising that remote sensing ET products predicts yield very well, as shown in analyses covering four sites in eastern Washington, USA (Khan et al., 2019), or 33 districts in the Czech Republic (Jurečka et al., 2021). Nevertheless, most large-scale statistical analyses of crop yields use precipitation and temperature as explanatory variables and ET has so far been overlooked as yield predictor over large areas.

While photosynthesis is impaired by water stress and suboptimal temperature at all growing stages (Fahad et al., 2017), other effects of hydroclimatic conditions on crop yields depend on the crop developmental phase at which they occur. Water stress and high temperatures during vegetative phases can impede root growth, affecting water and nutrient uptake (Calleja-Cabrera et al., 2020) and, consequently, reduce yield. Conversely, during and after reproductive phases, such adverse conditions impair yield maturation, and result in lower grain kernel number and biomass (Boyer and Westgate, 2004; Li et al., 2022; Soba et al., 2022). These phase-specific sensitivity to adverse conditions depend on the crop. Rice is more sensitive to heat stress during the vegetative than early reproductive phase (Cheabu et al., 2018), whereas corn, soybean and wheat yields are more sensitive to both water and heat stress in the reproductive than vegetative phase (Daryanto et al., 2016; Hamed et al., 2021; Hoffman et al., 2020). Understanding how hydroclimatic conditions affect yield variation requires examining their impact on the different, developmentally-relevant, parts of the growing season, in addition to the entire growing season. Nevertheless, most large-scale assessment of climatic impacts on yields focus on the entire growing season (e.g., Matiu et al., 2017; Ray et al., 2015; Vogel et al.,

2021) or short-term extreme conditions, such as dry and warm spells (Luan et al., 2021), irrespective of their timing in relation to the developmental phase. It remains unclear how hydroclimatic conditions determine yields by distinctly affecting plant during their developmental phases over large areas.

In addition to climatic conditions, crop yields are affected by soil properties. Soil texture impacts plant growth and grain yields (Sene et al., 1985; Nyéki et al., 2017) and influences all aspects of the soil water balance (Rodríguez-Iturbe and Porporato, 2005). For instance, infiltration in the rooting zone is higher and soil water evaporation lower in sandy soils compared with clayey soils. As a result, in dry climates, where soil moisture and hence infiltration are often low, precipitation is more effectively stored in coarse- than fine-textured soils (Noy-Meir, 1973), leading to higher primary production (Sala et al., 1988)—the so-called “inverse texture hypothesis.” Conversely, in wetter climates, this effect is reversed because the higher infiltration below the rooting zone of coarser soils removes water and nutrients from the root zone and is not compensated by lower evaporation, leading to lower production in coarse-textured soils. In parallel, higher bulk density—i. e., lower porosity—can reduce root penetration and length, soil moisture retention, and infiltration capacity, with the latter increasing runoff and leading to less plant-available water in the root zone (Horton et al., 1989; Houlbrooke et al., 1997; Zhang et al., 2006). In addition to its effects on hydrological properties, soil organic matter provides nutrients essential for plant growth, so, all else being equal, we expect that higher or more stable yields occur in soils rich in organic matter (Ma et al., 2023), which tend to have lower bulk density and thus higher water storage capacity (Rawls et al., 2003). As hydroclimatic and edaphic factors, and possibly their interaction, impact yields, they should be considered for yield prediction. Indeed, they are key inputs for crop-model yield simulations at various spatial scales and resolutions (Constantin et al., 2019; Hoffmann et al., 2016; Kuhnert et al., 2017; Maharjan et al., 2019). However, statistical analyses of observed yield have considered the combination of hydroclimatic and edaphic conditions only in small-scale contexts (Juhos et al., 2015; H. Liu et al., 2022). Over large climatic and geographic gradients, yield variability was explained by climatic controls (Li and Troy, 2018; Luan et al., 2021; Rosenzweig et al., 2014) or soil properties (He et al., 2014; Whalley et al., 2008) alone, neglecting their potential interactions. We thus lack large scale explorations of the interactive effects of edaphic and hydroclimatic conditions on crop yields.

To fill this gap, we quantify crop yield variations in response to interacting edaphic and hydroclimatic conditions, for irrigated rice and rainfed corn, soybean, spring wheat and winter wheat across the continental USA. We analyze to what extent yields are explained by precipitation (P) and temperature (T) and their interactions, or ET, of the entire growing season or developmentally relevant parts of it, as well as the role of soil sand content (SC) and bulk density (BD). We hypothesized that (a) ET can explain crop yield variations equally, or better than P and T, (b) yields are more sensitive to hydroclimatic conditions during distinct phases of the growing season rather than across the entire growing season, and (c) edaphic conditions modify hydroclimatic impacts on crop yields in addition to directly impacting yields. To test our hypotheses, we compare the explanatory power of yield variations of statistical models accounting for P, T, and their interactions, with models considering ET, and investigate the combined influence of soil properties on both models, during the entire growing season and before

and after flowering/silk emergence.

2. Method

2.1. Data acquisition and processing

County-level yield data for corn, rice, soybean, spring wheat and winter wheat across the conterminous United States were downloaded from the [United States Department of Agriculture \(USDA\) \(2022\)](#). We focused on counties where (a) the crop-specific planted area was at least 10 % of the total county land area, to ensure the crop was well represented within the county, and (b) the irrigated agricultural area was less than 10 % of the planted area, to reduce the effects of irrigation (for details refer to Supplementary Information (SI), section S1.1.3). Since rice is only irrigated, and grown in relatively few counties, it was excluded from both criteria in the aforementioned selection process. The number of counties included ranged from 46 for rice to 598 for soybean.

Monthly P and T data were obtained from the Climatic Research Unit Time-Series monthly high-resolution gridded multivariate climate data, v4 ([Harris et al., 2020](#)). Two ET products were compared: the Simplified Surface Energy Balance Actual Evapotranspiration (ETS) ([Senay et al., 2013; Velpuri et al., 2013](#)), and the actual evapotranspiration from the ERA5-Land hourly data (ETE) ([Muñoz-Sabater, 2019](#)). The two ET data were estimated via different methods (see SI Section S1.1.1) and are moderately correlated (Figs. S1, S23-S27).

To determine plant developmental phases ([Section 2.2](#)), we used daily 30-year average (1991–2020) accumulated growing degree days (AGDD) data available from the [USA National Phenology Network \(USA-NPN\) \(2023\)](#). Two versions with 32 °F (corresponding to 0 °C) base temperatures was used for winter wheat, and that with 50 °F (corresponding to 10 °C) for the other crops, matching commonly base temperatures of the different crops.

Bulk density (BD) and sand content (SC; i.e., fraction with 50–2000 µm particle size) relative to 60 cm depth were retrieved at 100 m spatial resolution ([Ramcharan et al., 2018](#)). As sand content and bulk density change slowly through time, they were considered time-invariant. Soil organic matter content was not included, as it is strongly negatively correlated to BD ([Federer et al., 1993; Prévost, 2004](#)).

Monthly P, T, ET and time invariant data on soil properties were spatially aggregated to county-level croplands (SI section S1.2). The analyses were restricted to 2000–2019 to match the period for which all the hydroclimatic data were available.

2.2. Crop growing season and development phases

For each spring crop, the growing season (GS) was defined as the period (months) between the median sowing and harvesting dates for the US state in which the county is located ([USDA, 2010](#)). For winter wheat, we focused on the *main* growing season, assumed to extend over the five months before the median harvest date.

The growing season was further split into two developmental phases (DP), before and after flowering (or silk emergence for corn). Specifically, DP1 included the months between the beginning of the (*main*) growing season and flowering, and DP2 included the months between flowering and the end of the growing season. In other words, the month of flowering was included in both DP1 and DP2.

For each county, we determined the average day of the year (DOY) of the crop flowering/silking as the day in which the accumulated growing degree days (AGDD) from sowing reached previously observed crop-specific thresholds (AGDD*; [Table 1](#)).

In the [USA-NPN \(2023\)](#) AGDD data, growing degree days are accumulated from January 1st, so adjustments were needed to determine the AGDD relative to the crop, determining the accumulated growing degree from sowing rather than January 1st. For spring-sown crops, the sowing date always occurs after January 1st, i.e., the AGDD relative to January 1st needs to be reduced by the AGDD from January 1st to the sowing

Table 1

Developmental phases used to split the growing season of each crop and its corresponding accumulated growing degree days from sowing (AGDD_c*) and base temperatures used for AGDD calculations.

Crop	Developmental phases	AGDD _c * (°C)	Base temperature (°C)	Reference
Corn	Silks emerging/ pollen shedding	1400	10	(Neild and Newman, 1990)
Rice	Flowering	≈1400 ^a	10	(Yang et al., 2020)
Soybean	Flowering (full bloom)	625	10	(Irmak and Sandhu, 2023)
Spring wheat	Flowering	1075	10	(USDA, 2023)
Winter wheat	Flowering	1075	0	(USDA, 2023)

^a Average of multiple AGDD values in the original sources.

date, i.e.,

$$AGDDsc_{x,t} = AGDD_{x,t} - AGDD_{x,MSD} \quad (1)$$

Conversely, autumn-sown crops are always sown before January 1st, i.e., the AGDD relative to January 1st needs to be augmented by the AGDD between the sowing date and the end of the calendar year, i.e.,

$$AGDDwc_{x,t} = AGDD_{x,t} + (AGDD_{x,365} - AGDD_{x,MSD}) \quad (2)$$

In [Eq. 1 and 2](#), spring and winter crops are denoted by *sc* and *wc*, respectively, and

- $AGDDsc_{x,t}$ and $AGDDwc_{x,t}$ are the AGDD for spring and winter crop, respectively, aggregated at county cropland *x* and day *t* of the year
- $AGDD_{x,t}$ is the AGDD from the [USA-NPN \(2023\)](#) data, relative to the crop-specific base temperature, aggregated at county cropland *x* and day *t* of the year
- $AGDD_{x,MSD}$ is the AGDD from the [USA-NPN \(2023\)](#) data, relative to the crop base temperature, aggregated at county cropland *x* and state-wide median sowing DOY for the crop
- $AGDD_{x,365}$ is the AGDD from the [USA-NPN \(2023\)](#) data, relative to the crop base temperature, aggregated at county cropland *x* and relative to the last day of the year (DOY 365)

The DOY of the developmental phase DP for crop *c* and county *x* was taken as the first DOY in which $AGDDsc_{x,t}$ or $AGDDwc_{x,t}$ (Eqs. [1 and 2](#)) equals or exceeds the threshold AGDD for the developmental phase and crop (AGDD_c*; [Table 1](#)). We set the month in which the developmental phase occurs as the month of the DOY when $AGDDsc_{x,t}$ and $AGDDwc_{x,t}$ exceed AGDD_c* if this DOY is in the first 14 days of the month, or the following month if this DOY is after the 14th of the month.

P and ET were cumulated, and T averaged, over the three growing periods: the entire growing season (GS), and before and after flowering/silking (DP1 and DP2, respectively).

2.3. Linear mixed-effect models

Linear mixed-effect (LME) models were used to analyze the yield data. We ran a total of 90 model formulations ([Table 2](#)): 5 crops × 3 variants of hydroclimatic predictors (P and T, ETS, or ETE) × 3 growing periods (GS, DP1, or DP2) × 2 variants of soil properties (BD vs SC). As fixed hydroclimatic effects, we considered P, T and their interactions ([Eq. 3](#)) or either one of the two ET products (ETE or ETS) alone ([Eq. 4](#)). The quadratic dependence on each variable was included as fixed effect because hydroclimatic conditions often affect yields non-linearly ([Leng and Huang, 2017; Luan et al., 2022; Proctor et al., 2022; Schlenker and Roberts, 2006, 2009; Zhang et al., 2022](#)). Regarding edaphic conditions,

Table 2

Summary of model variants and figures where results for each variant are shown. All variants were run with data from the entire growing season or the two sub-seasonal growing periods. P: precipitation, T: temperature, ETE and ETS: actual evapotranspiration from two methods (SI section 1.1.1), SC: sand content, BD: bulk density.

Model	Hydro-climatic factors	Soil factors	Equation	Figures
P and T models	P, T	–	3 ($\alpha_7 = \alpha_8 = 0$)	–
		SC	3 ($SP = SC$)	1, 2a, 4a, 4b, 5, 3a, S6a, S9a, S12
		BD	3 ($SP = BD$)	5, S4a, S5a, S7a, S8a, S8b, S10a, S11, S12
ETE models	ETE	–	4 ($\beta_4 = \beta_5 = 0$)	–
		SC	4 ($SP = SC$)	1, 2b, 4c, 6 3b, S6b, S9b
		BD	4 ($SP = BD$)	S4b, S5b, S7b, S8c, S10b, S11, S13
ETS models	ETS	–	4 ($\beta_4 = \beta_5 = 0$)	–
		SC	4 ($SP = SC$)	1, 2c, 4c, 6, 3c, S6c, S9b
		BD	4 ($SP = BD$)	S4c, S5c, S7c, S8c, S10b, S11, S13

either SC or BD were considered as a yield predictor, alone and in interaction with P or ET, because of the relevance of soil properties in holding precipitation-derived water. In all models, time was included as a fixed continuous variable to account for trends in agricultural practices or technological advancements, as well as climatic changes during the study period. The county number was used as a random effect (Δ_k), to capture differences among counties in factors not accounted for by the fixed effects.

All the fixed effect variables were rescaled (SI, section S1.3) using min-max normalization (e.g. Dey et al., 2021; Marta et al., 2020; Zhang et al., 2019), with the quadratic terms being squared after normalization. For visualization purposes, we show the non-normalized variables in figures illustrating the regression results.

In summary, the yield Y was predicted using base models including P and T,

$$Y_{ijk} = \underbrace{\alpha_0}_{\text{intercept}} + \underbrace{\alpha_1 P_{ijk}^2 + \alpha_2 P_{ijk} + \alpha_3 T_{ijk}^2 + \alpha_4 T_{ijk} + \alpha_5 P_{ijk} * T_{ijk} + \alpha_6 t}_{\text{hydroclimatic factors}} + \underbrace{\alpha_7 S_k + \alpha_8 P_{ijk} * S_k}_{\text{soil factors}} + \underbrace{\Delta_k}_{\text{random intercept}} + \underbrace{\epsilon_{ijk}}_{\text{errors}} \quad (3)$$

or models including ET instead of P and T (ET estimated as either ETE or ETS),

$$Y_{ijk} = \underbrace{\beta_0}_{\text{intercept}} + \underbrace{\beta_1 ET_{ijk}^2 + \beta_2 ET_{ijk} + \beta_3 t}_{\text{hydroclimatic factors}} + \underbrace{\beta_4 S_k + \beta_5 ET_{ijk} * S_k}_{\text{soil factors}} + \underbrace{\Delta_k}_{\text{random intercept}} + \underbrace{\epsilon_{ijk}}_{\text{errors}} \quad (4)$$

In Eq. 3 and 4,

- Y_{ijk} is the yield for crop i , time j and county k
- α_0 and β_0 are the intercept terms
- $\alpha_1 - \alpha_8$ and $\beta_1 - \beta_5$ are the coefficients for the fixed effects
- P_{ijk} is the growing season or developmental phase precipitation for crop i , time j , and county k
- T_{ijk} is the growing season or developmental phase temperature for crop i , time j , and county k
- ET_{ijk} is the growing season or developmental phase ET (ETE or ETS) for crop i , time j , and county k
- t is time in years

- S_k is a time-invariant soil property (bulk density (BD) or sand content (SC)) for county k
- Δ_k is the time-invariant random intercept term for each county k
- ϵ_{ijk} is the error term for crop i , time j , and county k

As a term of comparison, we also considered the simplified case of models not including any soil property, i.e., Eq. 3 with $\alpha_7 = \alpha_8 = 0$ and Eq. 4 with $\beta_4 = \beta_5 = 0$.

The models were fitted using the Restricted Maximum Likelihood (REML) method with R (version 4.1.3) *lme4* (version 1.1.29) package (Bates et al., 2015). The main assumptions of LME models, namely the normality and homoscedasticity of errors, were confirmed by visual inspection of Q-Q plots and three residuals plots: residuals vs. normal distribution kernel density estimation plots, residuals vs. fitted values plots, and residual distribution by county.

To test our first hypothesis, we compared P and T models to ETE and ETS models across the growing season and developmental phase for each crop and soil variable, resulting in 30 model comparisons. Specifically, we computed the Akaike Information Criterion (AIC) to compare models (Akaike, 1974). For absolute values of explained variance, marginal and conditional R^2 were calculated (Nakagawa and Schielzeth, 2013). To test our second hypothesis, we compared the 5–95 % confidence intervals of the predicted yield sensitivity to climatic conditions in DP1, DP2 and the growing season. We obtained the confidence intervals by fitting our models to 2000 bootstrapped pseudo-replicates created by resampling our data, calculating the model-predicted yield changes in response to unitary changes in the climatic variables for each pseudo-replicate, and considering the 5th and 95th percentiles, under average climatic (P and T, or ET) and soil (SC or BD) conditions.

3. Results

3.1. Model performance and selection

ET models had higher performance (i.e., lower AIC) than P and T models in 67 %, and captured a higher fraction of yield variation (i.e., higher marginal R^2) in 60 % of model combinations (first five columns of Figs. 1 and S11). Compared with ETE, ETS had lower AIC in 63 % but higher marginal R^2 only in 47 % of the model combinations (last five columns of Figs. 1 and S11). Altogether, the P and T models and ET models explained up to 77–87 % of yield variation depending on crop, as evidenced by the conditional R^2 (Figs. 2, 3, S4–7).

P and T during the entire growing season explained yield variations better than P and T in the two sub-seasonal periods for all crops except spring wheat when considering BD as soil property, and winter wheat when considering SC or BD (compare marginal R^2 values in Figs. 2, 3, S4, and S5 (a) to S6 and S7 (a)). P and T during DP1 explained a larger yield variation than during DP2 for all crops except corn (Figs. 2, 3, S4–5). Yield variation was explained better by ETE during DP1 for rice, spring wheat and winter wheat, by ETE during DP2 for corn, and by ETE of the growing season for soybean (Figs. 2, 3, S4–7). ETS during DP1 explained the highest fraction of yield variation for rice and winter wheat, but ETS during DP2 explained corn and soybean yield variation best (Figs. 2, 3, S4–7). In all cases, including one soil property (sand content, SC, or soil bulk density, BD) improved the model performance and described variation, based on both AIC and R^2 (not shown). We thus comment only on the models including a soil property.

3.2. Precipitation and temperature effects on yields

In all growing periods, model-predicted yields peaked at intermediate precipitation for all crops except rice, as indicated by negative P_{DP1}^2 , P_{DP2}^2 and P_G^2 coefficients (Figs. 2, 3, S4–10). Notably, spring wheat yields were lowered by reduced precipitation during DP1 (Figs. 4 and S8 (a)) and the entire growing season (Figs. S9–10 (a)), but were enhanced by reduced precipitation during DP2 (Figs. 4 and S8 (b)). For set

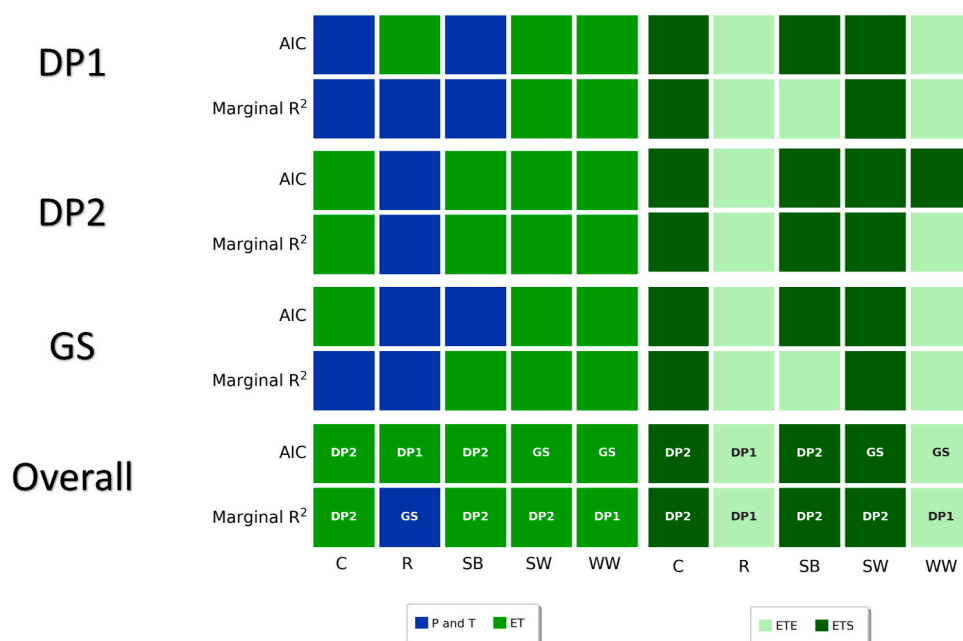


Fig. 1. Akaike Information Criterion (AIC) and marginal R² comparisons between models where precipitation (P) and temperature (T) or actual evapotranspiration (ET) are used as fixed effects. Colors indicate which of the model formulations had the highest performance (lowest AIC or highest marginal R²) when using climatic conditions during different periods (compare rows in pairs: growing season: GS; first plant development phase: DP1; second plant development phase: DP2) and overall (two bottom rows). In the first five columns, comparisons refer to P and T vs ET as predictors, with blue indicating that the P and T model is superior to the best of the ET models (ETS or ETE), and with green indicating that at least one of the ET models performs better than the P and T model. The last five columns compare models using the two ET products, with light green indicating that ETE is superior to ETS. All models include sand content as the soil variable. Crops are: corn (C), rice (R), soybean (SB), spring wheat (SW), and winter wheat (WW).

precipitation and soil property, cooler growing seasons improved the yields of all crops except soybean and winter wheat (Figs. S9, S10).

Yields were most sensitive to precipitation during DP2 or DP1, rather than the entire growing season. Based on model predictions at mean sand content, precipitation and temperature, the yield sensitivity to precipitation (as absolute value) was highest in DP2 for corn, soybean, and spring wheat (Table S5). For example, the yield increase in corn per unit precipitation increase for DP2 was 0.0047 ton ha⁻¹ mm⁻¹ (5 % to 95 % confidence interval (CI): 0.0044 to 0.0049), which is higher than that of DP1 or the growing season (0.0023; CI: 0.0020 to 0.0026 ton ha⁻¹ mm⁻¹ for DP1; and 0.0036; CI: 0.0033 to 0.0038 ton ha⁻¹ mm⁻¹ for the growing season). The yield sensitivity to precipitation was highest in DP1 and lowest in DP2 in winter wheat and rice, although the sign of the response differed (Table S5). Conversely, the period with highest yield sensitivity to temperature depended on the crop. The yield sensitivity was most negative in DP2 for soybean, and wheat varieties, but more negative in the growing season than DP1 for corn and rice (Table S6).

For given P and T, model-predicted yields were higher in fine- than coarse-textured soils, in all growing periods and crops, except rice and spring wheat (Fig. 5, blue vs. orange lines). Moreover, the precipitation at which yield peaked based on the model results – hereafter yield-maximizing precipitation – was lower in coarse-textured soils for most crops and growing periods (Fig. S12). The largest reduction in yield-maximizing precipitation occurred in winter wheat when considering the entire growing season – from 605 to 545 mm for SC increasing from 14 to 37 % (one standard deviation below and above the mean respectively). Higher bulk density corresponded to higher yield-maximizing precipitation for most growing periods for soybean and spring wheat, and in DP1 for corn (Fig. S12).

3.3. Actual evapotranspiration effects on yields

Crop yields changed non-linearly with ET (Figs. 2–4, S4–10). Under

mean SC and BD, model-predicted yields increased with growing season or sub-seasonal ETE for all crops except rice, although spring wheat yield started to decrease above ETE_{GS} ~ 400 mm, ETE_{DP1} ~ 350 mm, and ETE_{DP2} ~ 200 mm (Figs. 4 (c), S9 (b)). Rice yields decreased with increasing growing season or sub-seasonal ETE.

Yields were or tended to be most sensitive to ET during DP1 or DP2, instead of the entire growing season, for all crops and irrespective of ET products (Tables S7, S8). For example, at average ETE and SC, yields were most sensitive to ETE changes in DP1 for rice, spring wheat and winter wheat (–0.0038 ton ha⁻¹ mm⁻¹ for rice, 0.0059 ton ha⁻¹ mm⁻¹ for spring wheat and 0.0066 ton ha⁻¹ mm⁻¹ for winter wheat), while corn yield was more sensitive to ETE in DP2 than DP1 (Table S7). When considering ETS, corn, soybean and spring wheat yields were most sensitive to changes during DP2 (0.0178 ton ha⁻¹ mm⁻¹ for corn, 0.0057 ton ha⁻¹ mm⁻¹ for soybean and spring wheat; Table S8), whereas winter wheat yields were most sensitive to ETS changes during DP1 (0.0053 ton ha⁻¹ mm⁻¹).

Model-predicted winter wheat and corn yields were higher in fine-compared with coarse-textured soils at ETE_{GS} higher than 300 and 640 mm, respectively, but lower at low ETE (solid lines in Fig. 6). Rice and spring wheat yields were higher for any ETE in coarser soils, whereas soybean and winter wheat yields were higher in finer soils (Fig. 6). When considering ETS as predictor, corn, soybean, and spring wheat yields were generally higher in fine textured soils at high ETS, and in sandy soils at low ETS (dashed lines in Fig. 6). At all ETS values, winter wheat yields were higher and rice yields lower in fine- than coarse-textured soils (Fig. 6).

Regarding bulk density, using ETE as predictor, rice yields were higher in soils with high bulk density, whereas spring wheat and winter wheat yields were higher at low bulk density (Fig. S13). Corn yields were higher in soils with high bulk density, but only at ETE_{GS}, ETE_{DP1} and ETE_{DP2} above 675, 375 and 500 mm, respectively. Models using ETS generally predicted higher yields in low bulk density soils, with the exception of rice, and soybean predicted with ETE_{DP2} (Fig. S13).

	C	R	SB	SW	WW	
(a)	P_{DP1}^2	-0.77	0.29	-0.52	-0.61	-0.68
	P_{DP1}	0.54	-0.40	0.22	0.66	0.76
	T_{DP1}^2	-1.32	-0.30	-1.27	-0.17	-0.28
	T_{DP1}	0.92		1.37		0.30
	$P_{DP1}:T_{DP1}$	0.50		0.46	0.15	
	SC					
	$P_{DP1}:SC$	-0.23		-0.07		-0.13
	Time	0.20	0.25	0.21	0.13	0.05
	$R^2 (M) = 0.30$ $R^2 (C) = 0.65$ $\Delta AIC = 0.00$	$R^2 (M) = 0.39$ $R^2 (C) = 0.75$ $\Delta AIC = 6.11$	$R^2 (M) = 0.31$ $R^2 (C) = 0.68$ $\Delta AIC = 0.00$	$R^2 (M) = 0.19$ $R^2 (C) = 0.84$ $\Delta AIC = 97.08$	$R^2 (M) = 0.17$ $R^2 (C) = 0.74$ $\Delta AIC = 250.35$	
(b)	ETE_{DP1}^2		-0.30		-0.29	-0.17
	ETE_{DP1}	0.35		0.47	0.78	0.63
	SC	0.28			0.25	
	$ETE_{DP1}:SC$	-0.50		-0.22	-0.30	-0.15
	Time	0.18	0.23	0.19	0.11	0.07
		$R^2 (M) = 0.21$ $R^2 (C) = 0.57$ $\Delta AIC = 1381.83$	$R^2 (M) = 0.30$ $R^2 (C) = 0.74$ $\Delta AIC = 0.00$	$R^2 (M) = 0.27$ $R^2 (C) = 0.69$ $\Delta AIC = 948.83$	$R^2 (M) = 0.23$ $R^2 (C) = 0.82$ $\Delta AIC = 121.56$	$R^2 (M) = 0.25$ $R^2 (C) = 0.86$ $\Delta AIC = 0.00$
(c)	ETS_{DP1}^2	0.43	0.44	0.15	-0.61	-0.20
	ETS_{DP1}	0.21	-0.50	0.24	0.91	0.42
	SC	0.30		0.33		
	$ETS_{DP1}:SC$	-0.73		-0.60	-0.22	
	Time	0.19	0.22	0.21	0.11	0.06
		$R^2 (M) = 0.24$ $R^2 (C) = 0.67$ $\Delta AIC = 905.79$	$R^2 (M) = 0.25$ $R^2 (C) = 0.73$ $\Delta AIC = 30.63$	$R^2 (M) = 0.23$ $R^2 (C) = 0.72$ $\Delta AIC = 909.32$	$R^2 (M) = 0.25$ $R^2 (C) = 0.80$ $\Delta AIC = 0.00$	$R^2 (M) = 0.17$ $R^2 (C) = 0.80$ $\Delta AIC = 315.23$

Fig. 2. Heat maps showing coefficients for the fixed effects of the fitted models (Eq. 3 in a, Eq. 4 in b-c) for the first plant development phase (DP1), with sand content (SC) as soil property. Independent variables are shown in the rows: (a) linear, quadratic, and interaction terms for precipitation and temperature during the first plant development phase (P_{DP1} , and T_{DP1}), sand content (SC), and time; (b) and (c) same as in (a), but with actual evapotranspiration from the ERA5-Land hourly data or from the simplified surface energy balance during the first plant development phase (ETE_{DP1} or ETS_{DP1}), respectively. Crops are shown on the columns: corn (C), rice (R), soybean (SB), spring wheat (SW), and winter wheat (WW). Cells in red denote negative coefficients and cells in blue denote positive coefficients. Cells in gray represent coefficients with p -values higher than 0.05. Coefficients refer to effects of a unitary change of the normalized variable (Eq. 3 and 4) and are thus non-dimensional and comparable. Marginal (M) and conditional (C) R^2 for each model, and the difference between each model and the model with the lowest AIC (ΔAIC) are reported at the bottom of each column, with $\Delta AIC = 0$ denoting the best models for each crop.

4. Discussion

Our precipitation and temperature and actual evapotranspiration models explained up to 85 and 87 % of crop yields' variation, respectively (highest conditional R^2 for precipitation and temperature models and actual evapotranspiration models across Figs. 2, 3, S4–7), with an important contribution of county as random factor (similarly to Luan et al., 2021; Xu and Wu, 2018). Up to 46 % of yield variation was explained by the hydroclimatic and edaphic conditions and their interactions alone, i.e., without considering the random effects (Fig. S7). Therefore, regional-scale pedoclimatic conditions were important to explain yield variation regardless of county-specific factors. All crop

yields increased through time (Fig. 2, 3, S4–7), suggesting that improvements of agronomic practices (Ritchie and Roser, 2020) more than compensated any negative effects of climatic trends over the period explored (2000–2019). In the following, we discuss climate and soil effects without considering these long-term trends.

4.1. Actual evapotranspiration explains yield variation better than precipitation and temperature

Models using actual evapotranspiration as predictor performed better, based on AIC, than precipitation and temperature models, irrespective of the included soil factor (Figs. 1 and S11), thus supporting our

	C	R	SB	SW	WW	
(a)	P_{DP2}^2	-0.45		-0.65		-0.44
	P_{DP2}	0.76		0.71		0.52
	T_{DP2}^2	-0.61		-0.65	-0.22	-0.36
	T_{DP2}	0.32		0.50		0.35
	$P_{DP2}:T_{DP2}$			0.12	-0.21	-0.18
	SC					
	$P_{DP2}:SC$	-0.33		-0.15		
Time	0.18	0.24	0.19	0.12	0.06	
	$R^2 (M) = 0.30$	$R^2 (M) = 0.33$	$R^2 (M) = 0.30$	$R^2 (M) = 0.16$	$R^2 (M) = 0.08$	
	$R^2 (C) = 0.63$	$R^2 (C) = 0.74$	$R^2 (C) = 0.69$	$R^2 (C) = 0.80$	$R^2 (C) = 0.71$	
	$\Delta AIC = 1724.56$	$\Delta AIC = 0.00$	$\Delta AIC = 1668.03$	$\Delta AIC = 90.01$	$\Delta AIC = 451.02$	
(b)	ETE_{DP2}^2			-0.40	-0.57	-0.28
	ETE_{DP2}	0.66		1.10	0.75	0.60
	SC	0.43		0.20		
	$ETE_{DP2}:SC$	-0.68		-0.45		-0.16
	Time	0.16	0.22	0.19	0.12	0.06
	$R^2 (M) = 0.32$	$R^2 (M) = 0.27$	$R^2 (M) = 0.31$	$R^2 (M) = 0.20$	$R^2 (M) = 0.15$	
	$R^2 (C) = 0.69$	$R^2 (C) = 0.72$	$R^2 (C) = 0.73$	$R^2 (C) = 0.84$	$R^2 (C) = 0.75$	
	$\Delta AIC = 2133.89$	$\Delta AIC = 17.39$	$\Delta AIC = 1860.29$	$\Delta AIC = 167.15$	$\Delta AIC = 76.93$	
(c)	ETS_{DP2}^2			-0.45	-0.34	-0.61
	ETS_{DP2}	1.08		1.13	0.70	0.79
	SC	0.65	0.19	0.18		
	$ETS_{DP2}:SC$	-0.99		-0.39	-0.24	-0.16
	Time	0.18	0.22	0.20	0.10	0.06
	$R^2 (M) = 0.38$	$R^2 (M) = 0.20$	$R^2 (M) = 0.34$	$R^2 (M) = 0.27$	$R^2 (M) = 0.13$	
	$R^2 (C) = 0.80$	$R^2 (C) = 0.73$	$R^2 (C) = 0.81$	$R^2 (C) = 0.80$	$R^2 (C) = 0.79$	
	$\Delta AIC = 0.00$	$\Delta AIC = 32.20$	$\Delta AIC = 0.00$	$\Delta AIC = 0.00$	$\Delta AIC = 0.00$	

Fig. 3. Same as Fig. 2 but for developmental phase DP2. Soil property is sand content (SC).

first hypothesis. Furthermore, despite the lower number of parameters, actual evapotranspiration models captured a larger fraction of the yield variation for most crops, compared with precipitation and temperature models (higher conditional and marginal R^2 ; Figs. 1–3, S4–7, and S11). For comparison, our actual evapotranspiration models explained 75 % of soybean yield variation, whereas previous models for the same region including not only temperature and precipitation, but also root zone soil moisture explained 70 % of its variation (Hamed et al., 2021). The explained variance was only slightly lower for corn (81 % compared with 86 %) and equal for soybean (81 %) to that captured by machine learning models using six indicators of hydroclimatic conditions in the same region: vapor pressure deficit, daily minimum and maximum temperature, precipitation, extreme degree days, and surface downwelling shortwave flux (Hoffman et al., 2020) (Fig. S5).

We attribute the difference in performance between models using actual evapotranspiration and models using precipitation and temperature to how these variables reflect growing condition constraints on crops, in particular water availability. Precipitation affects yields mostly

indirectly, through its role as input to the soil water balance. However, the plant available water depends also on soil water evaporation, plant water uptake, interception, and percolation below the rooting zone (Rodríguez-Iturbe and Porporato, 2005). Temperature affects evapotranspiration rates, but also leaf temperature and hence all plant processes. Together, plant available water and air temperature affect carbon fixation, growth, and ultimately grain yields. Conversely, there is a closer link between actual evapotranspiration and crop yields, because of the coupling between transpiration and carbon fixation via photosynthesis, which in turn drives biomass growth and yield (Bhatt and Hossain, 2019; Fang et al., 2021; Vico and Porporato, 2015). Moreover, actual evapotranspiration is more closely connected to soil moisture than precipitation, as wetter soil promotes both evaporation from the soil surface and transpiration (Rodríguez-Iturbe and Porporato, 2005; Verhoef and Gegea, 2014).

Due to such mechanistic links, potential evapotranspiration is used in process-based crop growth models (e.g. Hsiao et al., 2009). Actual evapotranspiration, in comparison, has rarely been used as explanatory

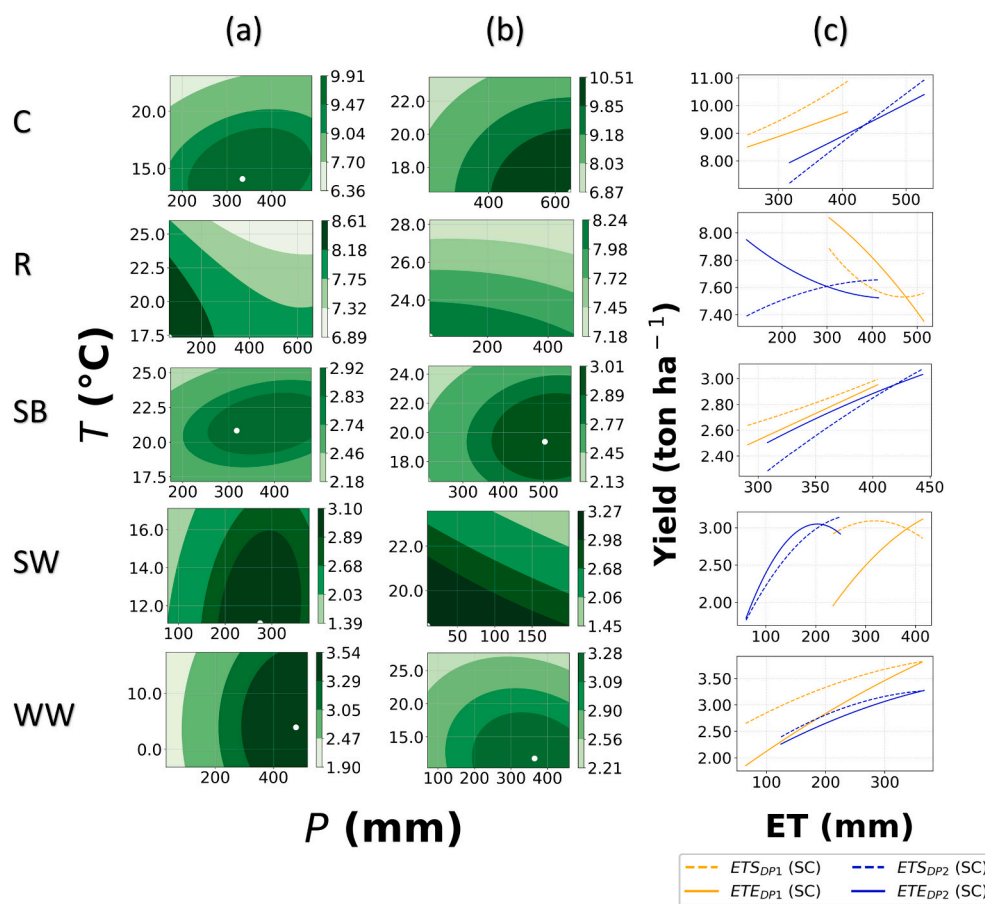


Fig. 4. Corn (C), rice (R), soybean (SB), spring wheat (SW) and winter wheat (WW) yield predictions using linear mixed effect models (LME) with precipitation (P) and temperature (T) as fixed effects (Eq. 3) during: (a) first plant development phase (DP1) and (b) second plant development phase (DP2), or (c) with actual evapotranspiration (ET) as fixed effect (Eq. 4) during the first and second plant development phases (blue and orange lines respectively). The predictions are based on the fixed effects only under average sand content and for year 2005, using non-normalized variables in the LME models. The white dots in (a) and (b) denote the conditions corresponding to the highest yield. The analysis was run on the entire range of observations, but the represented ranges of hydroclimatic conditions in the panels correspond to the 10th and 90th percentiles of observations.

variable for yield variations, and only for few growing seasons (Khan et al., 2019), or over comparatively limited hydroclimatic gradients (Jurečka et al., 2021– the Czech Republic), despite its increasing availability from remote sensing products. Given the pivotal role of water availability in plant development and in staving off water and heat stress, root-zone plant water availability would be the ideal yield predictor. Indeed, a global analysis showed that model estimates of root-zone soil moisture are more accurate predictors of yield than precipitation in corn, soybean, sorghum and millet and temperature in corn and sorghum (Proctor et al., 2022). However, root-zone soil moisture is hard to measure over large areas and would require accurate soil texture information to be transformed into plant available water. Here, we show that spatially-continuous actual evapotranspiration estimates can be an accurate alternative yield predictor.

Hydroclimatic conditions affected yields nonlinearly (Figs. 2–3). Increased growing season actual evapotranspiration were generally associated to improved yields, although winter wheat yield gains tapered off at high actual evapotranspiration and spring wheat yields declined at very high growing season actual evapotranspiration within the observed range (Figs. 6, S13). High actual evapotranspiration can occur because of high atmospheric evaporative demands, in turn associated with high temperatures, suggesting heat stress as one possible cause of yield decline at high actual evapotranspiration. However, high actual evapotranspiration could also stem from high soil moisture, enhancing soil water evaporation and, if extreme, causing damage from water logging and hypoxic/anoxic conditions as well as nutrient

leaching.

The difference of performance between the two actual evapotranspiration products was not substantial (Figs. 1–3, S4–7 and S11), mirroring findings from other analyses comparing actual evapotranspiration products (Jurečka et al., 2021). Nevertheless, for corn and soybean, post-flowering ETS models captured a larger fraction of yield variations than other periods, or in comparison to ETE (Figs. 2, 3, S4–7). Importantly, the same ETE and ETS values consistently predicted different yields in our models, indicating varying biases between the two estimates, possibly due to the different estimation approaches for actual evapotranspiration (SI section S1.1.1).

Similar to actual evapotranspiration, yields depended non-linearly on precipitation and temperature. Both excessively low and high precipitation reduced crop yields (Figs. 2 (a), 3 (a), S4–7 (a)), as previously observed (Leng and Huang, 2017; Luan et al., 2022; Schlenker and Roberts, 2009). Yields were likely reduced by water stress at low precipitation (Nguyen et al., 2023) and by cloudiness, wet conditions promoting pests and pathogens, delayed sowing or harvest (Ashraf and Habib-ur-Rehman., 1999; Li et al., 2019; Rosenzweig et al., 2002), water logging and associated limited oxygen and nutrient availability (Nguyen et al., 2018) at high precipitation. Our results for winter wheat confirm previously reported yield reductions under excess precipitation (W. Liu et al., 2022; Song et al., 2019) and dry conditions (Kukal and Irmak, 2018; Matiu et al., 2017) (Figs. 2, 3, S4–7, S9–10). As in previous estimates (Luan et al., 2022), warmer growing seasons improved soybean yields (Figs. S9–10).

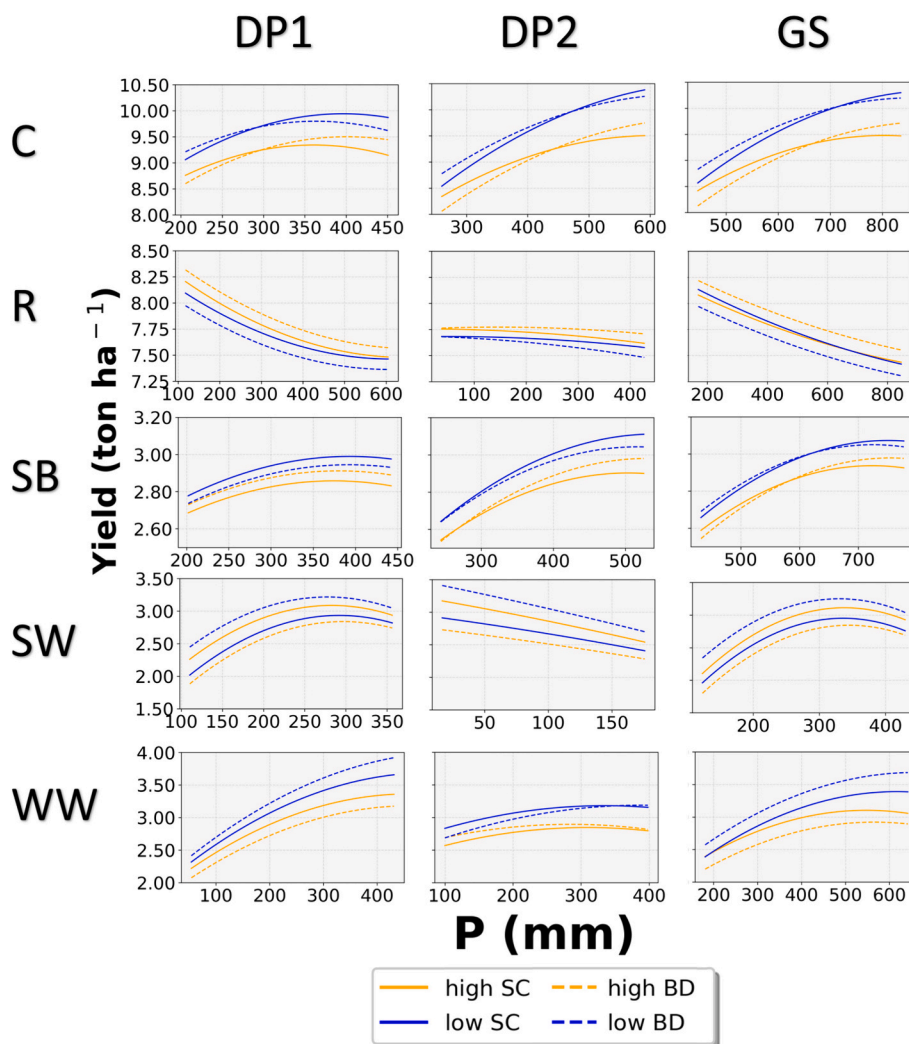


Fig. 5. Role of soil properties in mediating the yield response to precipitation, for set temperature. Corn (C), rice (R), soybean (SB), spring wheat (SW) and winter wheat (WW) yield predictions by linear mixed effect (LME) models including as fixed effects precipitation and temperature in the three growing periods (growing season: GS; first plant development phase: DP1; second plant development phase: DP2), under fixed temperature (mean of the observations for the growing period), and for low (blue) and high (orange) sand content (SC) (solid lines) and bulk density (BD) (dashed lines). Low and high SC and BD correspond to one standard deviation below and above the mean observation, respectively. The predictions are based on the fixed effects only, using non-normalized variables in the LME models; the year selected for these predictions was 2005. The analysis was run on the entire range of observations, but the represented ranges of climatic conditions in the panels correspond to the 10th and 90th percentiles of observations.

Rice yields were largely unaffected by hydroclimatic conditions (Figs. 2, 3, S4–7), as expected for an irrigated crop. Indeed globally, rice yields are less sensitive to hydroclimatic conditions compared with other crops (Heino et al., 2023), and irrigation in general alleviates heat and water stress (Luan et al., 2021). The emerging temperature dependence for rice yields (Figs. 4, S8–10) is likely influenced by the geographic distribution of data in our analyses, as the highest yielding counties are located in California, with growing season temperatures lower than 23 °C (see Fig. S19).

4.2. Yields were generally more sensitive to conditions during part of the growing season rather than the entire growing season

Yields were, or tended to be, more sensitive to changes in hydroclimatic conditions in part of the growing season compared with the entire season, with the exception of the effect of temperature on rice and corn yields, in line with our second hypothesis. Moreover, the best models for each crop based on AIC and marginal R^2 were mostly based on climatic conditions during either DP1 or DP2 rather than based on the entire growing season (Figs. 1, S11). Compared with before flowering

(DP1) or the entire growing season, conditions after flowering or silk emergence (DP2) had the largest effects on all crop yields except for rice in the case of precipitation, and except rice and corn for temperature. Indeed, previous pot and field experiments, and analyses of survey yield data found corn and soybean yields to be more affected by temperature and water stress during the reproductive phase, i.e. after flowering, compared with the vegetative phase (Hamed et al., 2021; Hoffman et al., 2020; Jumrani and Bhatia, 2018; Li et al., 2022). Conversely, the most sensitive period to ET changes depended on crop and ET product, suggesting that ET might capture both aspects of biomass accumulation during the vegetative phase (i.e., DP1) and the occurrence of detrimental conditions after flowering.

Interpretations of our results should consider uncertainties pertaining to the definition of the growing seasons and the development phases. First, we used state-wide median sowing and harvesting dates in defining the growing season for each county. This does not account for variations in growing seasons among counties within a state. Second, we use monthly temporal scales in defining both the growing season and its parts, as required for consistency with the scale of most hydroclimatic data. A finer temporal scale would enable more precise representation of

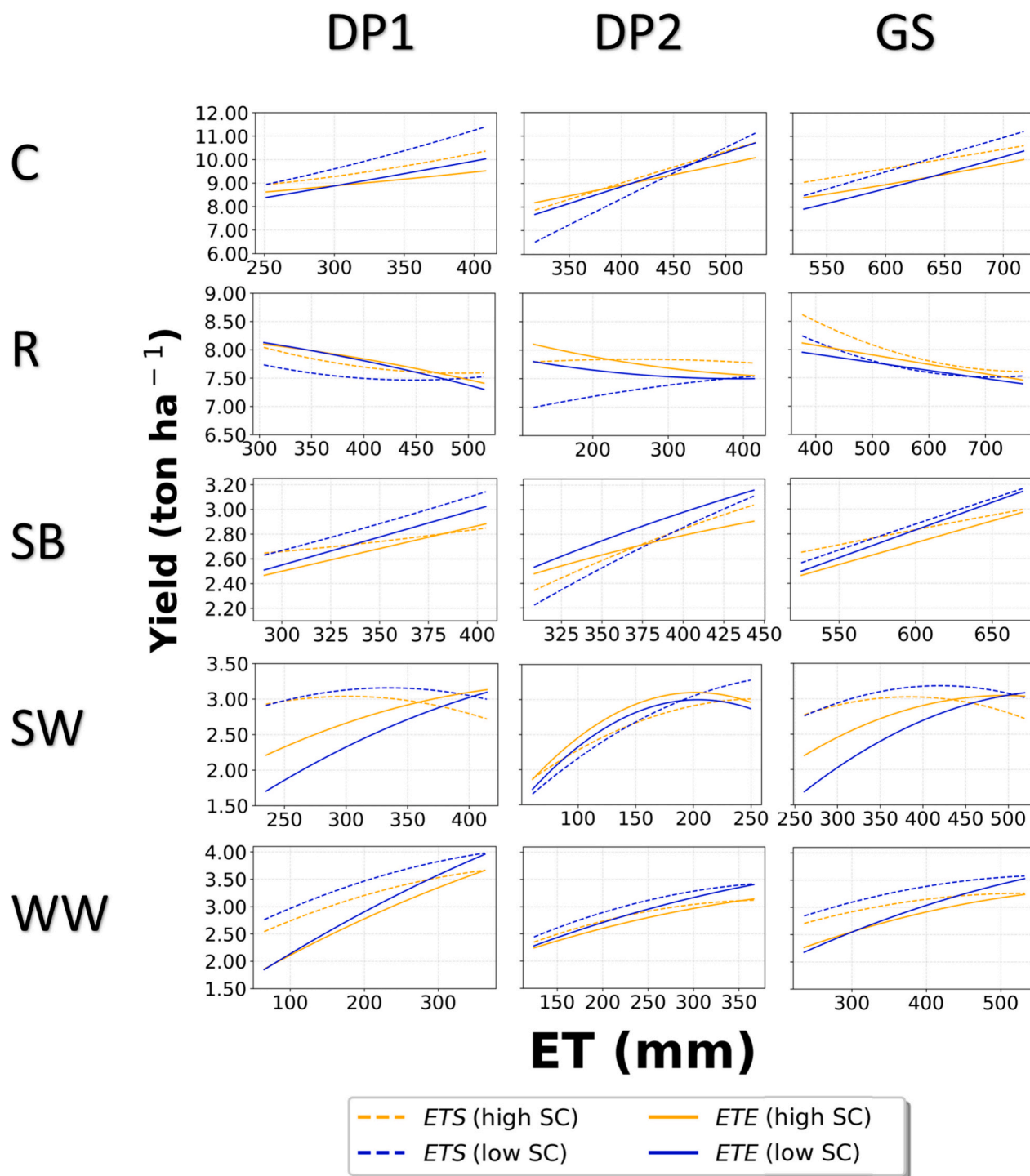


Fig. 6. Corn (C), rice (R), soybean (SB), spring wheat (SW) and winter wheat (WW) yield predictions from linear mixed effect (LME) models including as fixed effect evapotranspiration (Eq. 4), for ETS (dashed lines) and ETE (solid lines). Panels and symbols are as in Fig. 4: columns refer to the three growing periods (growing season: GS; first plant development phase: DP1; second plant development phase: DP2), line colors to low and high sand contents (SC) (blue and orange lines respectively). Time is set at the year 2005. The analysis was run on the entire range of observations, but the represented ET ranges correspond to the 10th and 90th percentiles of observations.

both the growing season and plant development phases. The month-long overlap between DP1 and DP2 was introduced to limit variations due to the coarse monthly separation and aggregation of sub-seasonal periods. Therefore, we expect our accumulated precipitation and actual evapotranspiration in both DP1 and DP2 to be somewhat overestimated. However, we do not expect this to affect our main findings, as confirmed by the similar results from studies in the same region with more precise

separation of intra-annual periods (e.g. Hoffman et al., 2020).

4.3. Soil properties interact with hydroclimatic impacts on crop yield

Confirming our third hypothesis, we found that sand content and bulk density modified crop yield predictions, directly by improving or suppressing yields, and indirectly by altering the hydroclimatic

conditions at which yield is maximized. When using precipitation and temperature as predictors, higher sand content reduced crop yields, with the exception of rice and spring wheat (Fig. 5).

High sand fraction reduces soil water and nutrient retention capacity and is associated with low soil fertility (Reichert et al., 2016; Huang and Hartemink, 2020), so it is not surprising that, regardless of precipitation, yields are often lower in coarser soils (Huang et al., 2021). The yield-maximizing precipitation during the growing season or during the development phases (DP1 and DP2) shifts to lower values in coarser soils for all crops except rice and spring wheat during the growing season, rice and winter wheat during DP1, and corn and spring wheat during DP2 (Figs. 6, S12). In other words, in coarser soils lower precipitation is sufficient to reach the maximum attainable yield, even though in most of the crops we considered the maximum yields in coarser soils are still lower than those in finer-textured soils. The lower yield-maximizing precipitation in coarser soils might be the result of their higher infiltration capacity, which partly offsets their higher percolation and nutrient leaching below the rooting zone, compared with fine-textured soils (Noy-Meir, 1973). While these water and nutrient losses in coarser soils likely make high precipitation less effective for crop growth (thus lowering yields), high infiltration rates allow yields to peak at relative low precipitation values—a result that we interpret as consistent with the inverse texture hypothesis (Noy-Meir, 1973; Sala et al., 1988). Coarser soils resulted in higher corn yields than finer soils in dry climates, whereas finer soils result in higher yields in wet climates based on a previous statistical analysis (Huang et al., 2021). Here, we find that corn yields were consistently lower in coarser soils when using precipitation as predictor. However, when using actual evapotranspiration (except ETS_{DP1}), corn yields in dry conditions (i.e., low actual evapotranspiration) were higher in coarser soils (Fig. 6), consistent with results by Sala et al. (1988) indicating higher productivity in coarser soils under dry conditions.

When using precipitation and temperature as predictors, high bulk density suppressed the yields of most crops (Fig. 5), likely by reducing soil penetrability by roots and hence root length, access to deeper water and nutrient resources, ultimately slowing down plant growth (Bengough et al., 2011; Houlbrooke et al., 1997; Young et al., 1997). High bulk density is also associated with lower soil organic matter (Rawls et al., 2003) and infiltration rate, and in general lower fertility. The model estimates point to higher precipitation needed to maximize the yields of corn (DP1), soybean (GS and DP2) and spring wheat (GS and DP1) in soils with high bulk density (Fig. S12). This result could be explained by high bulk density reducing root access to soil water (Houlbrooke et al., 1997) or water storage due to increased surface runoff in less permeable, compacted soil.

4.4. Implications for crop yields under climate change

We have shown that in most cases actual evapotranspiration had a higher explanatory power than more commonly employed climatic indices, like precipitation and temperature. Thus, actual evapotranspiration estimates can improve the evaluation of climate change impacts on crop production. As our analysis included several staple crops and a broad range of hydroclimatic conditions, we expect the higher performance of actual evapotranspiration to hold true in other parts of the world and potentially globally. Our results regarding actual evapotranspiration likely stem from its capacity to represent crop water use, i.e., the interplay between water availability and demands—a particularly important aspect in the face of more extreme climatic conditions.

Satellite-based and global actual evapotranspiration estimations are becoming increasingly available, and have the advantage of providing high resolution and spatially continuous information. However, limitations of these estimates, including the ones used here, are that they do not distinguish between the contributions of different crops to actual evapotranspiration or between transpiration and soil water evaporation, and are obtained from water and/or energy balance models and remote

sensing products at a scale too coarse to identify individual fields. In the context of our study not distinguishing evaporation and transpiration means that actual evapotranspiration during part of the pre-flowering period (i.e., in DP1) is likely to include a larger fraction of evaporation compared with later periods, when the canopy is closed. As we do not analyze yields at field scale, we expect that our approach of masking actual evapotranspiration per county cropland would provide sufficient level of granularity in spatial integration. Despite these limitations, actual evapotranspiration had a strong explanatory power of yields of a variety of crops.

The impact of hydroclimatic conditions on yields were mediated by soil properties (Figs. 2, 5, 6, S12). Our results suggest that soil properties can lower or raise the negative effects of climate change on crop yields. For example, it indicates that the detrimental effects of drier growing seasons on yields are raised under unfavorable soil conditions (i.e. in coarser and more compacted soils). As such, not including soil effects in predictive models of crop yields will under- or over-estimate climate change impacts. Moreover, while sand content is defined by topographic position and parent material, bulk density is also affected by soil and crop management. Reducing tillage or modifying its depth, controlling machinery traffic, adding organic matter to the soil, and more diverse crop rotation all could lower bulk density (Jones et al., 1989). Our results indicate that such practices will not only improve yields by lowering bulk density, but will also reduce the growing season and intra-seasonal precipitation required to achieve maximum yields. These practices are especially important since bulk density affects soil water holding capacity, which in turn can reduce yield volatility and stabilize it against dry spells and heatwaves (Williams et al., 2016).

5. Conclusion

For a variety of staple crops across the USA, we show that remotely sensed actual evapotranspiration explains yield variation better than precipitation and temperature, that yields are more sensitive to hydroclimatic impacts in crop-specific, phenologically-relevant parts of the growing season rather than the entire growing season, and that these impacts are modulated by edaphic conditions (sand content and bulk density). Yields improved with increasing growing season evapotranspiration, although spring wheat yields started to decline at high evapotranspiration. In general, yields were most sensitive to hydroclimatic conditions after flowering or silk emergence. Compared with coarser soils, higher yields occurred over finer soils under most climatic conditions, but yields were maximized at higher precipitation in finer soils and in soils with higher bulk density. These results highlight the importance of accounting for climate-soil synergetic effects when exploring the role of climatic conditions on yields. As actual evapotranspiration integrates soil moisture dynamics and crop water use that in turn affect yields, it can be utilized for large-scale, accurate yield predictions.

Funding

This work was supported by the Swedish Research Council for Sustainable Development (FORMAS) (grants 2018-02872 and 2018-00425); the Swedish Research Councils (Vetenskapsrådet/FORMAS/SIDA) (grant 2016-06313); and the Bolin Centre for Climate Research (RA7).

CRedit authorship contribution statement

Mahmoud Suliman: Writing – original draft, Visualization, Methodology, Formal analysis, Data curation. **Anna Scaini:** Writing – review & editing, Supervision, Methodology. **Stefano Manzoni:** Writing – review & editing, Supervision, Methodology, Conceptualization. **Giulia Vico:** Writing – review & editing, Supervision, Methodology, Conceptualization.

Declaration of competing interest

The authors declare that they have no known competing financial interests or personal relationships that could have appeared to influence the work reported in this paper.

Data availability

All data used in this study are freely available, and sourced in the supplementary information (SI Section 1.1).

Acknowledgements

We thank Armen Kemanian (Pennsylvania State University) and two anonymous reviewers for their comments.

Appendix A. Supplementary data

Supplementary data to this article can be found online at <https://doi.org/10.1016/j.scitotenv.2024.175172>.

References

- Akaike, H., 1974. A new look at the statistical model identification. *IEEE Trans. Autom. Control* 19 (6), 716–723. <https://doi.org/10.1109/TAC.1974.1100705>.
- Allen, R.G., Pereira, L.S., Raes, D., Smith, M., 1998. Crop evapotranspiration: guidelines for computing crop water requirements. In: *FAO Irrigation and Drainage Paper (FAO)*, 56. https://scholar.google.com/scholar_lookup?title=Crop+evapotranspiration+Guidelines+for+computing+crop+water+requirements&author=Allen%2C+R.G.&publication_year=1998.
- Ashraf, M., Habib-ur-Rehman, 1999. Interactive effects of nitrate and long-term waterlogging on growth, water relations, and gaseous exchange properties of maize (*Zea mays* L.). *Plant Sci.* 144 (1), 35–43. [https://doi.org/10.1016/S0168-9452\(99\)00055-2](https://doi.org/10.1016/S0168-9452(99)00055-2).
- Bates, D., Mächler, M., Bolker, B., Walker, S., 2015. Fitting linear mixed-effects models using lme4. *J. Stat. Softw.* 67, 1–48. <https://doi.org/10.18637/jss.v067.i01>.
- Bengough, A.G., McKenzie, B.M., Hallett, P.D., Valentine, T.A., 2011. Root elongation, water stress, and mechanical impedance: a review of limiting stresses and beneficial root tip traits. *J. Exp. Bot.* 62 (1), 59–68. <https://doi.org/10.1093/jxb/erq350>.
- Bhatt, R., Hossain, A., 2019. Concept and consequence of evapotranspiration for sustainable crop production in the era of climate change. In: *Advanced Evapotranspiration Methods and Applications*. IntechOpen. <https://doi.org/10.5772/intechopen.83707>.
- Boyer, J.S., Westgate, M.E., 2004. Grain yields with limited water. *J. Exp. Bot.* 55 (407), 2385–2394. <https://doi.org/10.1093/jxb/erh219>.
- Brás, T.A., Seixas, J., Carvalhais, N., Jägermeyr, J., 2021. Severity of drought and heatwave crop losses tripled over the last five decades in Europe. *Environ. Res. Lett.* 16 (6), 065012. <https://doi.org/10.1088/1748-9326/abff04>.
- Calleja-Cabrera, J., Boter, M., Oñate-Sánchez, L., Pernas, M., 2020. Root growth adaptation to climate change in crops. *Front. Plant Sci.* 11, 544. <https://doi.org/10.3389/fpls.2020.00544>.
- Cheabu, S., Mounq-Ngam, P., Arikat, S., Vanavichit, A., Malumpong, C., 2018. Effects of heat stress at vegetative and reproductive stages on spikelet fertility. *Rice Sci.* 25 (4), 218–226. <https://doi.org/10.1016/j.rsci.2018.06.005>.
- Constantin, J., Raynal, H., Casellas, E., Hoffmann, H., Bindi, M., Doro, L., Eckersten, H., Gaiser, T., Grosz, B., Haas, E., Kersebaum, K.-C., Klatt, S., Kuhnert, M., Lewan, E., Maharjan, G.R., Moriondo, M., Nendel, C., Roggero, P.P., Specka, X., Berge, J.-E., 2019. Management and spatial resolution effects on yield and water balance at regional scale in crop models. *Agric. For. Meteorol.* 275, 184–195. <https://doi.org/10.1016/j.agrformet.2019.05.013>.
- Daryanto, S., Wang, L., Jacinthe, P.-A., 2016. Global synthesis of drought effects on maize and wheat production. *PLoS One* 11 (5), e0156362. <https://doi.org/10.1371/journal.pone.0156362>.
- Dey, S., Dey, A.K., Mall, R.K., 2021. Modeling long-term groundwater levels by exploring deep bidirectional long short-term memory using hydro-climatic data. *Water Resour. Manag.* 35 (10), 3395–3410. <https://doi.org/10.1007/s11269-021-02899-z>.
- Elert, E., 2014. Rice by the numbers: a good grain. *Nature* 514 (7524). <https://doi.org/10.1038/514550a>. Article 7524.
- Fahad, S., Bajwa, A.A., Nazir, U., Anjum, S.A., Farooq, A., Zohaib, A., Sadia, S., Nasim, W., Adkins, S., Saud, S., Ihsan, M.Z., Alharby, H., Wu, C., Wang, D., Huang, J., 2017. Crop production under drought and heat stress: plant responses and management options. *Front. Plant Sci.* 8, 1147. <https://doi.org/10.3389/fpls.2017.01147>.
- Fang, H., Li, Y., Gu, X., Yu, M., Du, Y., Chen, P., Li, Y., 2021. Evapotranspiration partitioning, water use efficiency, and maize yield under different film mulching and nitrogen application in northwest China. *Field Crop Res.* 264, 108103. <https://doi.org/10.1016/j.fcr.2021.108103>.
- Federer, C.A., Turcotte, D.E., Smith, C.T., 1993. The organic fraction–bulk density relationship and the expression of nutrient content in forest soils. *Can. J. For. Res.* 23 (6), 1026–1032. <https://doi.org/10.1139/x93-131>.
- Goyal, M.R., Harmsen, E.W. (Eds.), 2013. *Evapotranspiration: Principles and Applications for Water Management*. Apple Academic Press. <https://doi.org/10.1201/b15779>.
- Hall, C., Dawson, T.P., Macdiarmid, J.I., Matthews, R.B., Smith, P., 2017. The impact of population growth and climate change on food security in Africa: looking ahead to 2050. *Int. J. Agric. Sustain.* 15 (2), 124–135. <https://doi.org/10.1080/14735903.2017.1293929>.
- Hamed, R., Van Loon, A.F., Aerts, J., Coumou, D., 2021. Impacts of compound hot–dry extremes on US soybean yields. *Earth Syst. Dynam.* 12 (4), 1371–1391. <https://doi.org/10.5194/esd-12-1371-2021>.
- Harris, I., Osborn, T.J., Jones, P., Lister, D., 2020. Version 4 of the CRU TS monthly high-resolution gridded multivariate climate dataset. *Scientific Data* 7 (1). <https://doi.org/10.1038/s41597-020-0453-3>. Article 1.
- He, Y., Hou, L., Wang, H., Hu, K., McConkey, B., 2014. A modelling approach to evaluate the long-term effect of soil texture on spring wheat productivity under a rain-fed condition. *Sci. Rep.* 4 (1). <https://doi.org/10.1038/srep05736>. Article 1.
- Heino, M., Kinnunen, P., Anderson, W., Ray, D.K., Puma, M.J., Varis, O., Siebert, S., Kumm, M., 2023. Increased probability of hot and dry weather extremes during the growing season threatens global crop yields. *Sci. Rep.* 13 (1), 3583. <https://doi.org/10.1038/s41598-023-29378-2>.
- Hoffman, A., Kemanian, A., Forest, C., 2020. The response of maize, sorghum, and soybean yield to growing-phase climate revealed with machine learning. *Environ. Res. Lett.* 15 (9), 094013. <https://doi.org/10.1088/1748-9326/ab7b22>.
- Hoffmann, H., Zhao, G., Asseng, S., Bindi, M., Biernath, C., Constantin, J., Coucheny, E., Dechow, R., Doro, L., Eckersten, H., Gaiser, T., Grosz, B., Heinlein, F., Kassie, B.T., Kersebaum, K.-C., Klein, C., Kuhnert, M., Lewan, E., Moriondo, M., Ewert, F., 2016. Impact of spatial soil and climate input data aggregation on regional yield simulations. *PLoS One* 11 (4), e0151782. <https://doi.org/10.1371/journal.pone.0151782>.
- Horton, R., Allmaras, R.R., Cruse, R.M., 1989. Tillage and compactive effects on soil hydraulic properties and water flow. In: *Larson, W.E., Blake, G.R., Allmaras, R.R., Voorhees, W.B., Gupta, S.C. (Eds.), Mechanics and Related Processes in Structured Agricultural Soils*. Springer, Netherlands, pp. 187–203. https://doi.org/10.1007/978-94-009-2421-5_15.
- Houlbrooke, D.J., Thom, E.R., Chapman, R., McLay, C.D.A., 1997. A study of the effects of soil bulk density on root and shoot growth of different ryegrass lines. *N. Z. J. Agric. Res.* 40 (4), 429–435. <https://doi.org/10.1080/00288233.1997.9513265>.
- Hsiao, T.C., Heng, L., Steduto, P., Rojas-Lara, B., Raes, D., Fereres, E., 2009. AquaCrop—the FAO crop model to simulate yield response to water: III. Parameterization and testing for maize. *Agron. J.* 101 (3), 448–459. <https://doi.org/10.2134/agnonj2008.0218s>.
- Huang, J., Hartemink, A.E., 2020. Soil and environmental issues in sandy soils. *Earth Sci. Rev.* 208, 103295. <https://doi.org/10.1016/j.earscirev.2020.103295>.
- Huang, J., Hartemink, A.E., Kucharik, C.J., 2021. Soil-dependent responses of US crop yields to climate variability and depth to groundwater. *Agric. Syst.* 190 (C). <https://ideas.repec.org/a/eee/agisys/v190y2021ics0308521x2100038x.html>.
- Irmak, S., Sandhu, R., 2023. Soybean crop coefficients under different seeding rates and full and limited irrigation and rainfed management. *Irrig. Drain. n/a (n/a)*. <https://doi.org/10.1002/ird.2854>.
- Jones, A., Wiese, R., Dickey, E., 1989. *Management Strategies to Minimize and Reduce Soil Compaction*. Biological Systems Engineering: Papers and Publications. <https://digitalcommons.unl.edu/biosysengfacpub/263>.
- Juhos, K., Szabó, S., Ladányi, M., 2015. Influence of soil properties on crop yield: a multivariate statistical approach. *International Agrophysics* 29 (4), 433–440. <https://doi.org/10.1515/intag-2015-0049>.
- Jumrani, K., Bhatia, V.S., 2018. Impact of combined stress of high temperature and water deficit on growth and seed yield of soybean. *Physiol. Mol. Biol. Plants* 24 (1), 37–50. <https://doi.org/10.1007/s12298-017-0480-5>.
- Jurečka, F., Fischer, M., Hlavinka, P., Balek, J., Semerádová, D., Bláhová, M., Anderson, M.C., Hain, C., Zalud, Z., Trnka, M., 2021. Potential of water balance and remote sensing-based evapotranspiration models to predict yields of spring barley and winter wheat in the Czech Republic. *Agric. Water Manag.* 256, 107064. <https://doi.org/10.1016/j.agwat.2021.107064>.
- Katul, G.G., Oren, R., Manzoni, S., Higgins, C., Parlange, M.B., 2012. Evapotranspiration: a process driving mass transport and energy exchange in the soil–plant–atmosphere–climate system. *Rev. Geophys.* 50 (3). <https://doi.org/10.1029/2011RG000366>.
- Khan, A., Stöckle, C.O., Nelson, R.L., Peters, T., Adam, J.C., Lamb, B., Chi, J., Waldo, S., 2019. Estimating biomass and yield using METRIC evapotranspiration and simple growth algorithms. *Agron. J.* 111 (2), 536–544. <https://doi.org/10.2134/agnonj2018.04.0248>.
- Kuhnert, M., Yeluripati, J., Smith, P., Hoffmann, H., van Oijen, M., Constantin, J., Coucheny, E., Dechow, R., Eckersten, H., Gaiser, T., Grosz, B., Haas, E., Kersebaum, K.-C., Kiese, R., Klatt, S., Lewan, E., Nendel, C., Raynal, H., Sosa, C., Ewert, F., 2017. Impact analysis of climate data aggregation at different spatial scales on simulated net primary productivity for croplands. *Eur. J. Agron.* 88, 41–52. <https://doi.org/10.1016/j.eja.2016.06.005>.
- Kukul, M.S., Irmak, S., 2018. Climate-driven crop yield and yield variability and climate change impacts on the U.S. Great Plains agricultural production. *Sci. Rep.* 8 (1). <https://doi.org/10.1038/s41598-018-21848-2>. Article 1.
- Leng, G., Huang, M., 2017. Crop yield response to climate change varies with crop spatial distribution pattern. *Sci. Rep.* 7 (1), 1463. <https://doi.org/10.1038/s41598-017-01599-2>.

- Li, X., Troy, T.J., 2018. Changes in rainfed and irrigated crop yield response to climate in the western US. *Environ. Res. Lett.* 13 (6), 064031 <https://doi.org/10.1088/1748-9326/aac4b1>.
- Li, Y., Guan, K., Schnitke, G.D., DeLucia, E., Peng, B., 2019. Excessive rainfall leads to maize yield loss of a comparable magnitude to extreme drought in the United States. *Glob. Chang. Biol.* 25 (7), 2325–2337. <https://doi.org/10.1111/gcb.14628>.
- Li, T., Zhang, X., Liu, Q., Liu, J., Chen, Y., Sui, P., 2022. Yield penalty of maize (*Zea mays* L.) under heat stress in different growth stages: a review. *J. Integr. Agric.* 21 (9), 2465–2476. <https://doi.org/10.1016/j.jia.2022.07.013>.
- Liu, H., Colombi, T., Jäck, O., Keller, T., Weih, M., 2022. Effects of soil compaction on grain yield of wheat depend on weather conditions. *Sci. Total Environ.* 807, 150763 <https://doi.org/10.1016/j.scitotenv.2021.150763>.
- Liu, W., Sun, W., Huang, J., Wen, H., Huang, R., 2022. Excessive rainfall is the key meteorological limiting factor for winter wheat yield in the middle and lower reaches of the Yangtze River. *Agronomy* 12 (1). <https://doi.org/10.3390/agronomy12010050>. Article 1.
- Luan, X., Bommarco, R., Scaini, A., Vico, G., 2021. Combined heat and drought suppress rainfed maize and soybean yields and modify irrigation benefits in the USA. *Environ. Res. Lett.* 16 (6), 064023 <https://doi.org/10.1088/1748-9326/abfc76>.
- Luan, X., Bommarco, R., Vico, G., 2022. Coordinated evaporative demand and precipitation maximize rainfed maize and soybean crop yields in the USA. *Ecohydrology*. <https://doi.org/10.1002/eco.2500>.
- Ma, Y., Woolf, D., Fan, M., Qiao, L., Li, R., Lehmann, J., 2023. Global crop production increase by soil organic carbon. *Nat. Geosci.* 16 (12), 1159–1165. <https://doi.org/10.1038/s41561-023-01302-3>.
- Maharjan, G.R., Hoffmann, H., Webber, H., Srivastava, A.K., Weihermüller, L., Villa, A., Coucheney, E., Lewan, E., Trombi, G., Moriondo, M., Bindi, M., Grosz, B., Dechow, R., Kühnert, M., Doro, L., Kersebaum, K.-C., Stella, T., Specka, X., Nendel, C., Gaiser, T., 2019. Effects of input data aggregation on simulated crop yields in temperate and Mediterranean climates. *Eur. J. Agron.* 103, 32–46. <https://doi.org/10.1016/j.eja.2018.11.001>.
- Marta, E., Guglielmo, R., Giuliana, B., Alessandra, B., Veronica, V., Paola, M., 2020. Past and future hydrogeological risk assessment under climate change conditions over urban settlements and infrastructure systems: the case of a sub-regional area of Piedmont, Italy. *Nat. Hazards* 102 (1), 275–305. <https://doi.org/10.1007/s11069-020-03925-w>.
- Matui, M., Ankerst, D.P., Menzel, A., 2017. Interactions between temperature and drought in global and regional crop yield variability during 1961–2014. *PLoS One* 12 (5), e0178339. <https://doi.org/10.1371/journal.pone.0178339>.
- Muñoz-Sabater, J., 2019. ERA5-land hourly data from 1981 to present. In: Copernicus Climate Change Service (C3S) Climate Data Store (CDS). <https://doi.org/10.24381/cds.e2161bac>.
- Nakagawa, S., Schielzeth, H., 2013. A general and simple method for obtaining R2 from generalized linear mixed-effects models. *Methods Ecol. Evol.* 4, 133–142. <https://doi.org/10.1111/J.2041-210x.2012.00261.X>.
- Neild, R., Newman, J., 1990. Growing season characteristics and requirements in the corn belt. In: *National Corn Handbook*. Cooperative Extension Service, Purdue University. <https://www.extension.purdue.edu/extmedia/NCH/NCH04.html>.
- Nguyen, L., Osanal, Y., Anderson, I.C., Bange, M.P., Tissue, D.T., Singh, B.K., 2018. Flooding and prolonged drought have differential legacy impacts on soil nitrogen cycling, microbial communities and plant productivity. *Plant Soil* 431 (1–2), 371–387. <https://doi.org/10.1007/s11104-018-3774-7>.
- Nguyen, H., Thompson, A., Costello, C., 2023. Impacts of historical droughts on maize and soybean production in the southeastern United States. *Agric. Water Manag.* 281, 108237 <https://doi.org/10.1016/j.agwat.2023.108237>.
- Noy-Meir, I., 1973. Desert ecosystems: environment and producers. *Annu. Rev. Ecol. Syst.* 4, 25–51.
- Nyéké, A., Milics, G., Kovács, A.J., Neményi, M., 2017. Effects of soil compaction on cereal yield: a review. *Cereal Res. Commun.* 45 (1), 1–22. <https://doi.org/10.1556/0806.44.2016.056>.
- Prévost, M., 2004. Predicting soil properties from organic matter content following mechanical site preparation of Forest soils. *Soil Sci. Soc. Am. J.* 68 (3), 943–949. <https://doi.org/10.2136/sssaj2004.9430>.
- Proctor, J., Rigden, A., Chan, D., Huybers, P., 2022. More accurate specification of water supply shows its importance for global crop production. *Nature Food* 3 (9). <https://doi.org/10.1038/s43016-022-00592-x>. Article 9.
- Ramcharan, A., Hengl, T., Nauman, T., Brungard, C., Waltman, S., Wills, S., Thompson, J., 2018. Soil property and class maps of the conterminous US at 100 meter spatial resolution based on a compilation of national soil point observations and machine learning. *Soil Sci. Soc. Am. J.* 82 (1), 186–201. <https://doi.org/10.2136/sssaj2017.04.0122>.
- Rawls, W.J., Pachepsky, Y.A., Ritchie, J.C., Sobecki, T.M., Bloodworth, H., 2003. Effect of soil organic carbon on soil water retention. *Geoderma* 116 (1–2), 61–76. [https://doi.org/10.1016/S0016-7061\(03\)00094-6](https://doi.org/10.1016/S0016-7061(03)00094-6).
- Ray, D.K., Gerber, J.S., MacDonald, G.K., West, P.C., 2015. Climate variation explains a third of global crop yield variability. *Nat. Commun.* 6 (1) <https://doi.org/10.1038/ncomms6989>. Article 1.
- Reichert, J.M., Amado, T.J.C., Reinert, D.J., Rodrigues, M.F., Suzuki, L.E.A.S., 2016. Land use effects on subtropical, sandy soil under sandification/desertification processes. *Agric. Ecosyst. Environ.* 233, 370–380. <https://doi.org/10.1016/j.agee.2016.09.039>.
- Ritchie, H., Roser, M., 2020. Agricultural Production. *Our World in Data*. <https://ourworldindata.org/agricultural-production>.
- Rodríguez-Iturbe, I., Porporato, A., 2005. *Ecohydrology of Water-Controlled Ecosystems: Soil Moisture and Plant Dynamics*. Cambridge University Press. <https://doi.org/10.1017/CBO9780511535727>.
- Rosenzweig, C., Tubiello, F.N., Goldberg, R., Mills, E., Bloomfield, J., 2002. Increased crop damage in the US from excess precipitation under climate change. *Glob. Environ. Chang.* 12 (3), 197–202. [https://doi.org/10.1016/S0959-3780\(02\)00008-0](https://doi.org/10.1016/S0959-3780(02)00008-0).
- Rosenzweig, C., Elliott, J., Deryng, D., Ruane, A.C., Müller, C., Arneth, A., Boote, K.J., Folberth, C., Glotter, M., Khabarov, N., Neumann, K., Piontek, F., Pugh, T.A.M., Schmid, E., Stehfest, E., Yang, H., Jones, J.W., 2014. Assessing agricultural risks of climate change in the 21st century in a global gridded crop model intercomparison. *Proc. Natl. Acad. Sci.* 111 (9), 3268–3273. <https://doi.org/10.1073/pnas.1222463110>.
- Sala, O.E., Parton, W.J., Joyce, L.A., Lauenroth, W.K., 1988. Primary production of the central grassland region of the United States. *Ecology* 69 (1), 40–45. <https://doi.org/10.2307/1943158>.
- Schlenker, W., Roberts, M.J., 2006. Nonlinear effects of weather on corn yields. *Rev. Agric. Econ.* 28 (3), 391–398.
- Schlenker, W., Roberts, M.J., 2009. Nonlinear temperature effects indicate severe damages to U.S. crop yields under climate change. *Proc. Natl. Acad. Sci.* 106 (37), 15594–15598. <https://doi.org/10.1073/pnas.0906865106>.
- Senay, G.B., Bohms, S., Singh, R.K., Gowda, P.H., Velpuri, N.M., Alemu, H., Verdin, J.P., 2013. Operational evapotranspiration mapping using remote sensing and weather datasets: a new parameterization for the SSEB approach. *JAWRA Journal of the American Water Resources Association* 49 (3), 577–591. <https://doi.org/10.1111/jawr.12057>.
- Sene, M., Vepraskas, M.J., Naderman, G.C., Denton, H.P., 1985. Relationships of soil texture and structure to corn yield response to subsoiling. *Soil Sci. Soc. Am. J.* 49 (2), 422–427. <https://doi.org/10.2136/sssaj1985.03615995004900020030x>.
- Soba, D., Arrese-Igor, C., Aranjuelo, I., 2022. Additive effects of heatwave and water stresses on soybean seed yield is caused by impaired carbon assimilation at pod formation but not at flowering. *Plant Sci.* 321, 111320 <https://doi.org/10.1016/j.plantsci.2022.111320>.
- Song, Y., Linderholm, H.W., Wang, C., Tian, J., Huo, Z., Gao, P., Song, Y., Guo, A., 2019. The influence of excess precipitation on winter wheat under climate change in China from 1961 to 2017. *Sci. Total Environ.* 690, 189–196. <https://doi.org/10.1016/j.scitotenv.2019.06.367>.
- United States Department of Agriculture (USDA), 2010. Economics, Statistics and Market Information System (ESMIS)—Usual Planting and Harvesting Dates for U.S. Field Crops. <https://usda.library.cornell.edu/concern/publications/vm40xr56k>.
- United States Department of Agriculture (USDA), 2022. National Agricultural Statistics Service—QuickStats Ad-hoc Query Tool. <https://quickstats.nass.usda.gov/>.
- United States Department of Agriculture (USDA), 2023. International Production Assessment Division (IPAD)—Metadata for Winter/Spring Wheat Growth Stage Models. <https://ipad.fas.usda.gov/cropexplorer/description.aspx?legendid=313®ionid=na>.
- USA National Phenology Network, 2023. Extended Accumulated Growing Degree Days Gridded Data Products. <https://doi.org/10.5066/F7SN0723>.
- Velpuri, N.M., Senay, G.B., Singh, R.K., Bohms, S., Verdin, J.P., 2013. A comprehensive evaluation of two MODIS evapotranspiration products over the conterminous United States: using point and gridded FLUXNET and water balance ET. *Remote Sens. Environ.* 139, 35–49. <https://doi.org/10.1016/j.rse.2013.07.013>.
- Verhoef, A., Egea, G., 2014. Modeling plant transpiration under limited soil water: comparison of different plant and soil hydraulic parameterizations and preliminary implications for their use in land surface models. *Agric. For. Meteorol.* 191, 22–32. <https://doi.org/10.1016/j.agrformet.2014.02.009>.
- Vico, G., Porporato, A., 2015. Ecohydrology of agroecosystems: quantitative approaches towards sustainable irrigation. *Bull. Math. Biol.* 77 (2), 298–318. <https://doi.org/10.1007/s11538-014-9988-9>.
- Vogel, J., Rivoire, P., Deidda, C., Rahimi, L., Sauter, C.A., Tschumi, E., van der Wiel, K., Zhang, T., Zscheischler, J., 2021. Identifying meteorological drivers of extreme impacts: an application to simulated crop yields. *Earth Syst. Dynam.* 12 (1), 151–172. <https://doi.org/10.5194/esd-12-151-2021>.
- Wang, Y., Zhang, Y., Yu, X., Jia, G., Liu, Z., Sun, L., Zheng, P., Zhu, X., 2021. Grassland soil moisture fluctuation and its relationship with evapotranspiration. *Ecol. Indic.* 131, 108196 <https://doi.org/10.1016/j.ecolind.2021.108196>.
- Whalley, W.R., Watts, C.W., Gregory, A.S., Mooney, S.J., Clark, L.J., Whitmore, A.P., 2008. The effect of soil strength on the yield of wheat. *Plant Soil* 306 (1), 237. <https://doi.org/10.1007/s11104-008-9577-5>.
- Williams, A., Hunter, M.C., Kammerer, M., Kane, D.A., Jordan, N.R., Mortensen, D.A., Smith, R.G., Snapp, S., Davis, A.S., 2016. Soil water holding capacity mitigates downside risk and volatility in US rainfed maize: time to invest in soil organic matter? *PLoS One* 11 (8), e0160974. <https://doi.org/10.1371/journal.pone.0160974>.
- Xu, H., Wu, M., 2018. A first estimation of county-based green water availability and its implications for agriculture and bioenergy production in the United States. *Water* 10 (2), 148. <https://doi.org/10.3390/w10020148>.
- Yang, C.-Y., Yang, M.-D., Tseng, W.-C., Hsu, Y.-C., Li, G.-S., Lai, M.-H., Wu, D.-H., Lu, H.-Y., 2020. Assessment of rice developmental stage using time series UAV imagery for variable irrigation management. *Sensors (Basel, Switzerland)* 20 (18), 5354. <https://doi.org/10.3390/s20185354>.
- Young, I.M., Montagu, K., Conroy, J., Bengough, A.G., 1997. Mechanical impedance of root growth directly reduces leaf elongation rates of cereals. *New Phytol.* 135 (4), 613–619. <https://doi.org/10.1046/j.1469-8137.1997.00693.x>.

- Zhang, S., Grip, H., Lövdahl, L., 2006. Effect of soil compaction on hydraulic properties of two loess soils in China. *Soil Tillage Res.* 90, 117–125. <https://doi.org/10.1016/j.still.2005.08.012>.
- Zhang, R., Chen, Z.-Y., Xu, L.-J., Ou, C.-Q., 2019. Meteorological drought forecasting based on a statistical model with machine learning techniques in Shaanxi province, China. *Sci. Total Environ.* 665, 338–346. <https://doi.org/10.1016/j.scitotenv.2019.01.431>.
- Zhang, T., He, Y., DePauw, R., Jin, Z., Garvin, D., Yue, X., Anderson, W., Li, T., Dong, X., Zhang, T., Yang, X., 2022. Climate change may outpace current wheat breeding yield improvements in North America. *Nat. Commun.* 13 (1) <https://doi.org/10.1038/s41467-022-33265-1>. Article 1.